

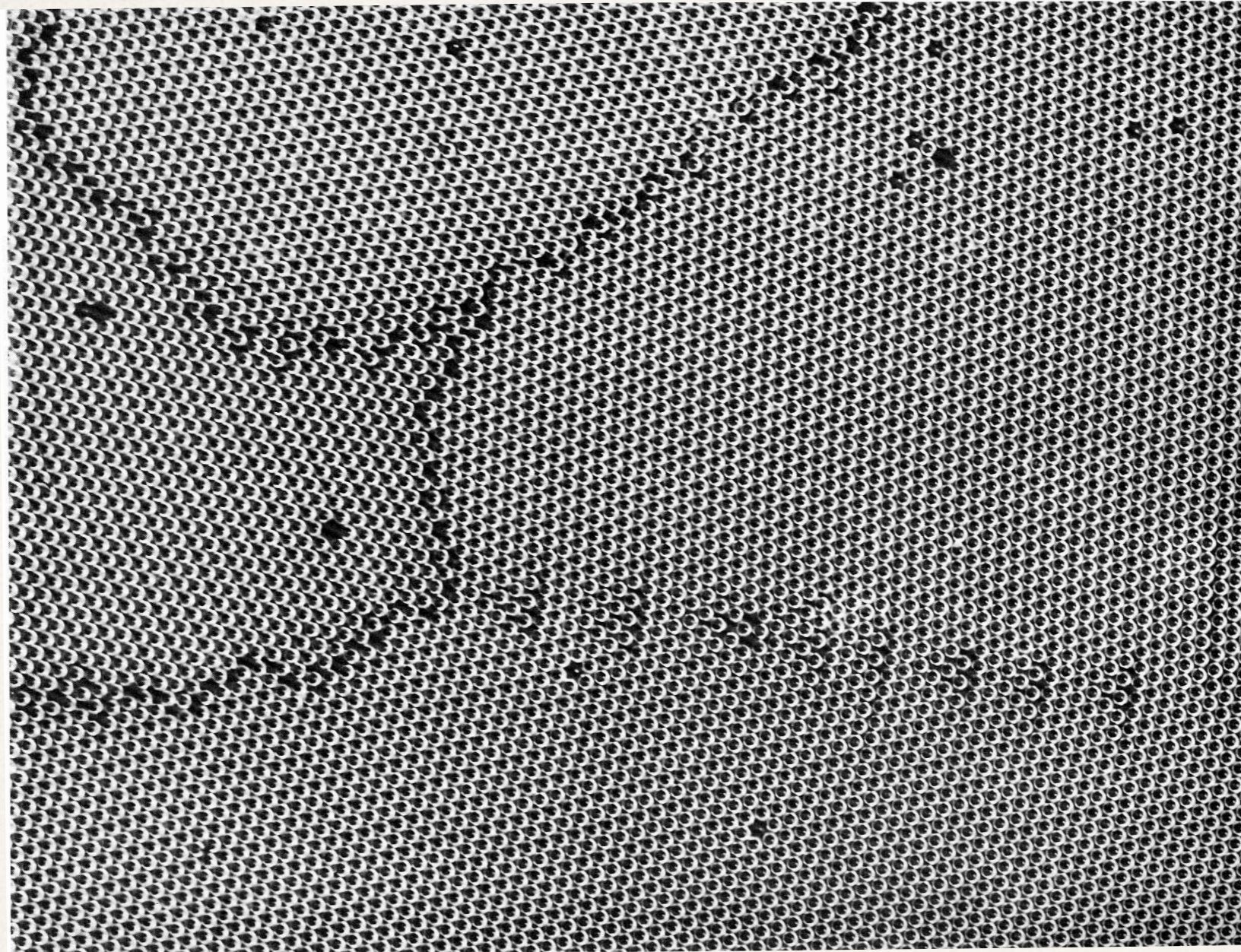
Kinetic equations for grain boundary networks in two-dimensions

Govind Menon (Brown University)

Joint work with:

Joe Klobusicky (Geisinger Health Systems),
Bob Pego (Carnegie Mellon University)

"Grain boundaries" in soap bubbles



Structure, Substructure, Superstructure,
Cyril Smith, Rev. Modern. Phys (1964)

Grain boundary networks

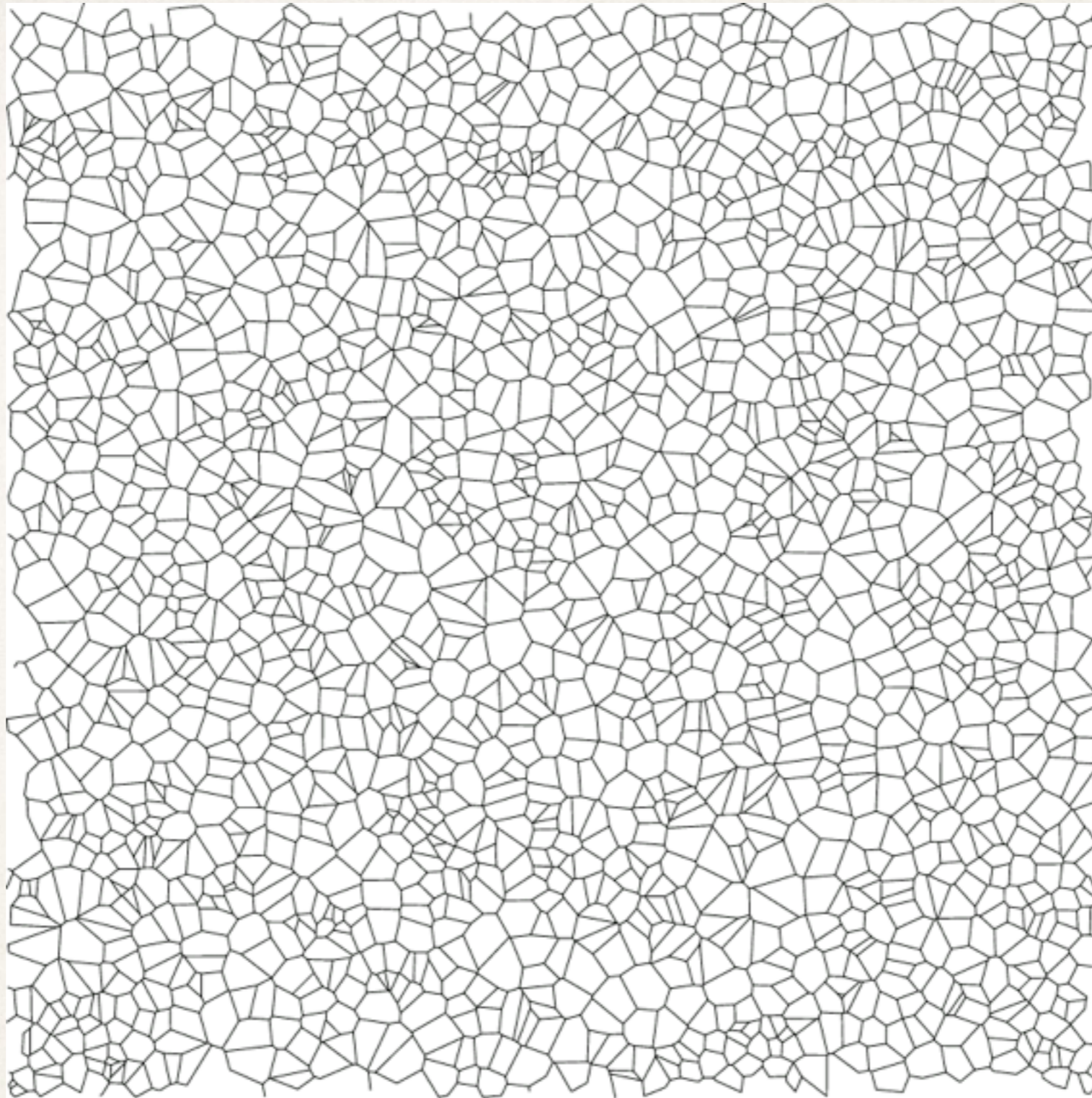
In the simplest approximation, the microstructure of a 2D polycrystalline material is described by a cellular network consisting of polygonal cells (grains) and their boundaries.

The energy of the system is the perimeter of the grain boundaries.

Each grain boundary evolves by motion by mean curvature+ the Herring boundary condition. This means that the grain boundaries meet at vertices where the line tensions must be in equilibrium.

Typically these are trivalent, symmetric vertices, except at singular times, when edges or cells shrink to zero size.

2D simulations



Evolution of a random network by motion by mean-curvature + Herring boundary condition. (Courtesy: Emanuel Lazar).

Some fundamental facts

The von Neumann-Mullins' relation (1951): the rate of change of area of a grain with k sides, depends only on its topology (number of edges, k), not on its geometry (e.g. length of the sides).

$$\frac{dA_k}{dt} = k - 6.$$

The above relation means, in particular, that grains with fewer than six sides must vanish, and the network must coarsen. That is, the number of grains must decrease, and the typical size of grains must increase.

Empirically, the area of a typical domain grows linearly in time. In fact, the microstructure is seen to be "statistically self-similar"!

J. VON NEUMANN

DISCUSSION

Written Discussion: By John von Neumann, Institute for Advanced Study, Princeton, N. J.

The considerations that follow deal with the changes of bubble-volume due to diffusion, that occur in a two-dimensional bubble-froth (a "Flat Cell"), as shown in Fig. 12 of Dr. C. S. Smith's paper (to be quoted as "G.L."). As pointed out on page 79, G.L., such changes of volume are due to the diffusion of the gas that fills the bubbles, through the liquid film that forms the (separating) bubble-walls. This diffusion is caused by the pressure difference between adjacent cells (cf. loc. cit. above). In first approximation it is proportional to this pressure difference. To be more precise: The diffusion-flow across a particular bubble-wall is (in the approximation referred to above) proportional to the pressure difference between the two bubbles adjacent to this wall, multiplied by the length of the wall.

The pressure difference of the two adjacent bubbles, at a given point P of a wall, is $2\gamma/R$, where γ is the surface tension of the liquid forming the froth, and R is the radius of curvature of the wall at P (cf. page 77, G.L.). γ is constant throughout the froth. Let P move over one wall-side, i.e., one side separating two given bubbles. Then these two bubbles and their respective pressures are fixed, hence the pressure difference between them is fixed, and so $2\gamma/R$ must be constant. R is therefore constant, i.e., the side in question is a circular arc. Each bubble is bounded by a polygon formed of circular arcs.

Consider such an arc, of radius R and angular aperture α . The pressure difference across it is $2\gamma/R$, the length of the arc is $R\alpha$. Hence the diffusion flow across this arc (wall-side) is proportional to $2\gamma/R \cdot R\alpha = 2\gamma\alpha$, i.e., to α .

Consider next a bubble in its entirety. Let the bounding circular-arc-polygon have n sides. These sides are circular arcs; let their angular apertures be $\alpha_1, \dots, \alpha_n$, respectively. Let the angle between sides i and i+1 (side n+1 is side 1) be θ_i , i.e., the angles are $\theta_1, \dots, \theta_n$, respectively. Actually each $\theta_i = 120^\circ = 2\pi/3$ (cf. page 75, G.L.), but this is not relevant yet.

Replace each arc by its chord, then an ordinary (rectilinear) polygon obtains. The replacement of arc i by its chord increases each adjacent polygonal angle by $\frac{1}{2}\alpha_i$. Hence θ_i is increased by $\frac{1}{2}\alpha_{i-1} + \frac{1}{2}\alpha_i$. The corresponding external angle of the rectilinear polygon obtains by complementing this to $180^\circ = \pi$, i.e., it is $\pi - \theta_i - \frac{1}{2}\alpha_{i-1} - \frac{1}{2}\alpha_i$. The sum of all external angles of the rectilinear polygon is $360^\circ = 2\pi$, i.e.,

$$\sum (\pi - \theta_i - \frac{1}{2}\alpha_{i-1} - \frac{1}{2}\alpha_i) = 2\pi,$$

$$n\pi - \sum \theta_i - \sum \alpha_i = 2\pi,$$

and, using $\theta_i = \frac{2\pi}{3}$ (cf. above),

$$\frac{n}{3}\pi - \sum \alpha_i = 2\pi,$$

$$\sum \alpha_i = \frac{n-6}{3}\pi.$$

Now it was pointed out, above, that the diffusion-flow across the side is proportional to α_i . Note that α_i may be > 0 as well as < 0 . $\alpha_i > 0$ (< 0) means that the side in question is convex (concave); hence the bubble in question loses (gains) gas across this side by diffusion. (Cf. Fig. 10, G.L.) Thus the diffusion-flow's proportionality to α_i holds even with respect to the signs (i.e., the coefficient of proportionality is positive), if the flow is interpreted as a rate of loss of gas.

In this sense, then, the total diffusion flow of a bubble, i.e., its total gas-loss-rate, is (positively) proportional to $\sum \alpha_i = \frac{n-6}{3}\pi$ (cf. above), i.e., to $n-6$. Or, equivalently:

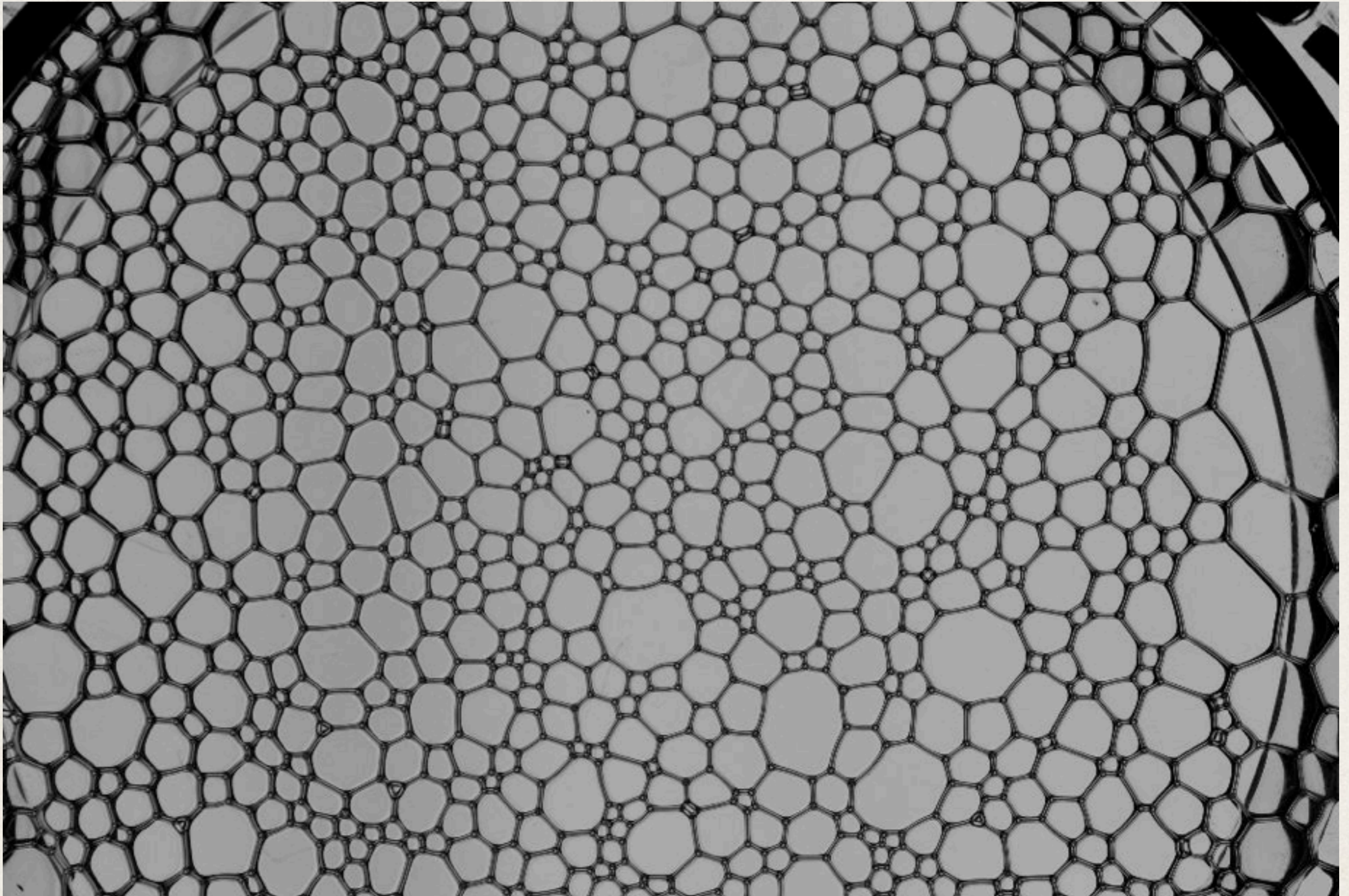
In a two-dimensional bubble-froth the total gas-gain-rate of any bubble is (positively) proportional to $n-6$, where n is the number of sides of the bubble (i.e., of its bounding circular-arc-polygon). The (positive) coefficient of proportionality depends only on the general properties of the froth and of its containing "Flat Cell".

Thus every hexagonal bubble (irrespective of further details of shape) has a constant-gas-content, every pentagonal bubble loses gas at the same rate; every heptagonal bubble gains gas at the same rate as the pentagonal ones lose it; every tetragonal (octagonal) bubble loses (gains) gas at twice the rate at which pentagonal (heptagonal) bubbles lose (gain) it, etc.

Note, that these results apply only to the continuous changes of gas-content due to diffusion. There remains the problem of finding a comparably simple characterization of the total changes of bubble-shapes due to these changes of gas-content. There remains, also, the problem of doing the same for the discontinuous changes that occur when a side disappears (cf. pages 78, 79, G.L.). Finally, these results are valid in two, but not in three, dimensions.

J. von Neumann (1951). Collected Papers, Vol. VI.

Physical experiments on soap bubbles



Experiments by Adam Roth (U.Penn), movie courtesy: Emanuel Lazar (U. Penn).

Recent work in applied math (1). Computation and modeling.

(1) Development and implementation of numerical schemes for the study of large networks.

Front tracking schemes 1.: Kinderlehrer, Lee,..., Ta'asan et al;

Front tracking schemes 2: Lazar, Srolovitz and Macpherson.

Level-set methods: Elsey, Esedoglu and Smereka;

Restricted gradient flows: Henseler, Niethammer, Otto.

(2) Reduced models: Barmak, Emelianenko, Epshteyn, ..., Kinderlehrer, Ta'asan-- use statistics obtained from computer simulation to develop simplified models for coarsening.

Recent work in applied math (2). Random topology 1.

MacPherson-Srolovitz formula in 3-dimensions (Nature, 2007)

$$\int_{\partial D} \kappa dA = 2\pi \left(\mathcal{L}(D) - \frac{1}{6} \sum_{i=1}^6 e_i(D) \right).$$

$\mathcal{L}(D)$ the "mean width" of a domain D.

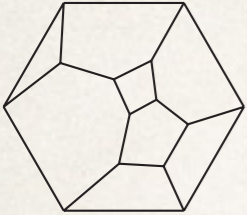
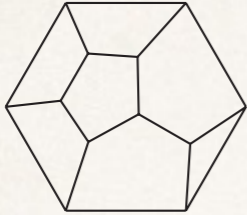
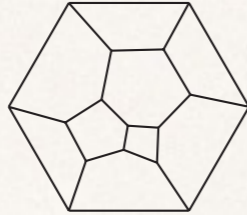
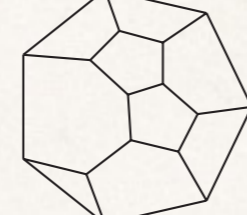
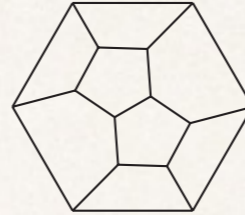
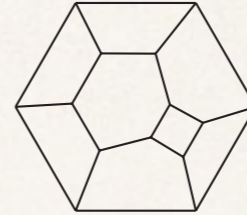
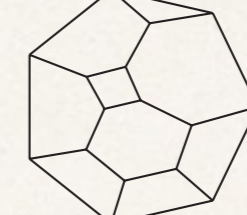
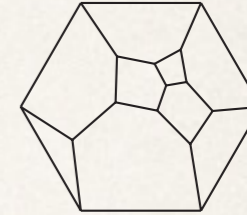
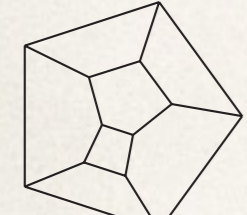
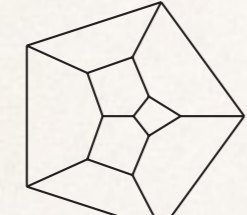
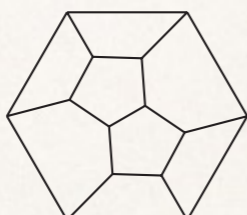
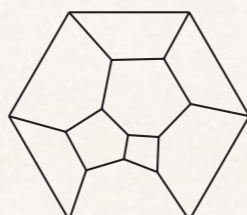
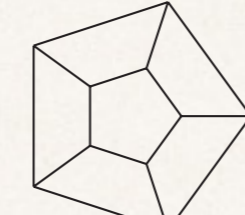
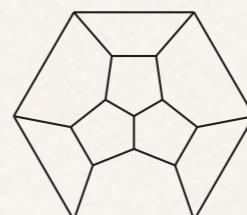
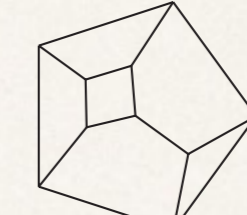
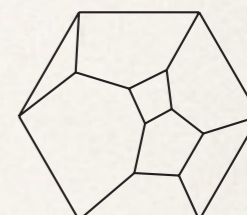
MacPherson-Srolovitz formula in d-dimensions (Nature, 2007)

$$\frac{d}{dt} \text{Vol}_d(D) = -2\pi \left(H_{d-2}(D_d) - \frac{1}{6} H_{d-2}(D_{d-2}) \right).$$

$\text{Vol}_d(D)$ d- dimensional Lebesgue measure of D.

$H_s(D_p)$ Hadwiger s-measure of p-dimensional feature of D.

Recent work in applied math (2). Random topologies in 3D

Poisson-Voronoi							
P1, $f=0.28\%$	P2, $f=0.17\%$	P3, $f=0.15\%$	P4, $f=0.13\%$	P5, $f=0.13\%$	P6, $f=0.10\%$	P7, $f=0.10\%$	P8, $f=0.10\%$
							
(00133200...) $F=9, S=1$	(00133100...) $F=8, S=2$	(00044200...) $F=10, S=2$	(00134110...) $F=10, S=1$	(00044100...) $F=9, S=4$	(00052200...) $F=9, S=4$	(00142210...) $F=10, S=1$	(00125200...) $F=10, S=2$
Grain growth							
G1, $f=2.83\%$	G2, $f=1.86\%$	G3, $f=1.63\%$	G4, $f=1.53\%$	G5, $f=1.48\%$	G6, $f=1.43\%$	G7, $f=1.39\%$	G8, $f=1.38\%$
							
(0004400...) $F=8, S=8$	(0003600...) $F=9, S=12$	(0004410...) $F=9, S=4$	(0004420...) $F=10, S=2$	(0005200...) $F=7, S=20$	(0003610...) $F=10, S=6$	(0013300...) $F=7, S=6$	(0013320...) $F=9, S=1$

Lazar, Mason, Macpherson, Srolovitz, *Phy. Rev. Lett.* (2012).

Our goal and results

Goal: to rigorously derive a kinetic theory for the coarsening of grain boundary networks.

Results:

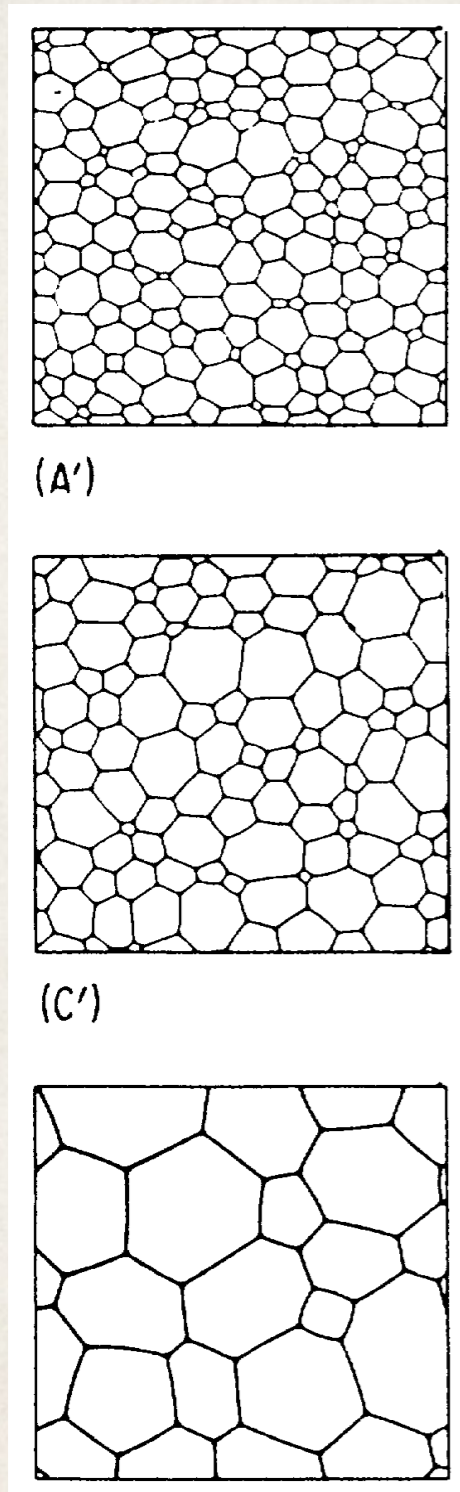
(a) Hydrodynamic limit theorem: rigorously derive kinetic equations from a particle system that is a cartoon of the evolution of grain sizes by von Neumann's rule, interspersed with random flips.

(Technically, this is more like a result in queuing theory, than geometric PDE and relies on the theory of piecewise deterministic Markov processes).

(b) Computational modeling: Simulation of particle system; derivation of parameters of the model from "full computations" by others.

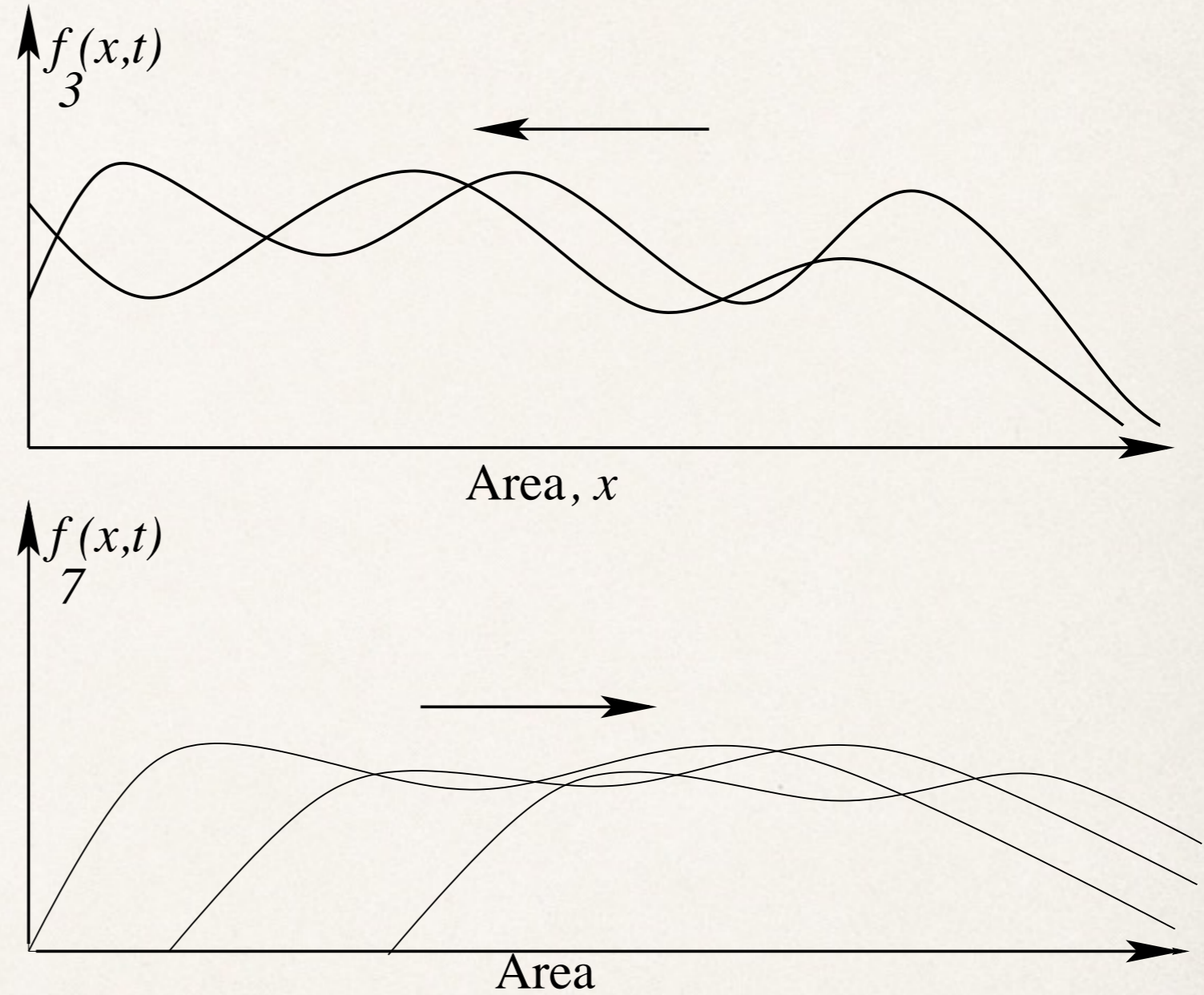
(c) Analysis of kinetic equations. For example, well-posedness and a proof of asymptotic self-similarity in some simple cases.

Random fields compared with kinetic description



Grain boundary evolution

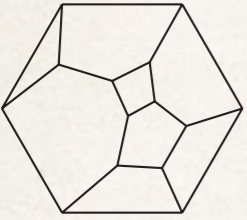
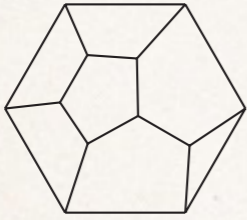
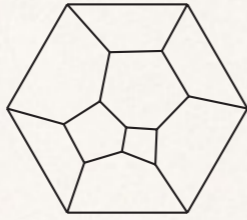
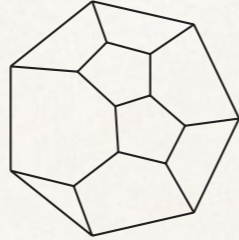
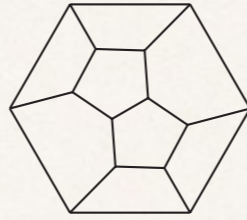
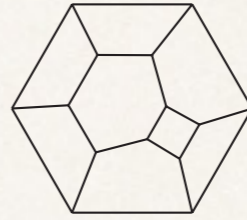
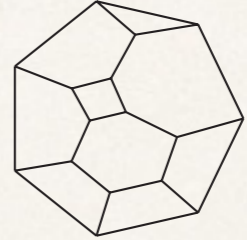
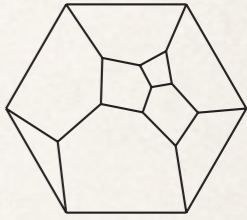
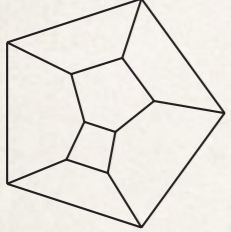
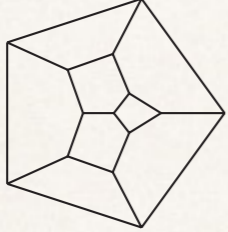
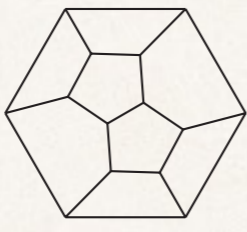
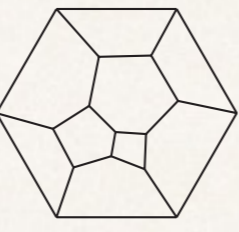
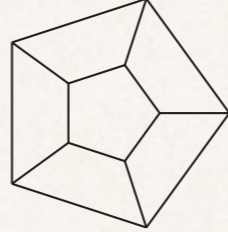
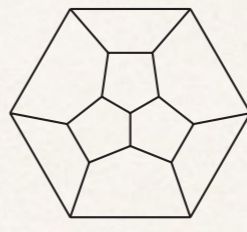
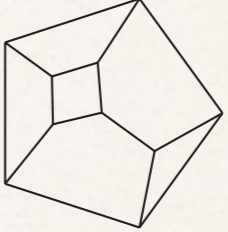
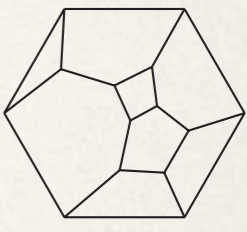
Figure: Flyvbjerg, Phys. Rev. E (1993)



Kinetic description

Flow of number densities of 3 and 7 grains

Topological types in 3D are much more complicated!

Poisson-Voronoi							
P1, $f=0.28\%$	P2, $f=0.17\%$	P3, $f=0.15\%$	P4, $f=0.13\%$	P5, $f=0.13\%$	P6, $f=0.10\%$	P7, $f=0.10\%$	P8, $f=0.10\%$
							
(00133200...) $F=9, S=1$	(00133100...) $F=8, S=2$	(00044200...) $F=10, S=2$	(00134110...) $F=10, S=1$	(00044100...) $F=9, S=4$	(00052200...) $F=9, S=4$	(00142210...) $F=10, S=1$	(00125200...) $F=10, S=2$
Grain growth							
G1, $f=2.83\%$	G2, $f=1.86\%$	G3, $f=1.63\%$	G4, $f=1.53\%$	G5, $f=1.48\%$	G6, $f=1.43\%$	G7, $f=1.39\%$	G8, $f=1.38\%$
							
(0004400...) $F=8, S=8$	(0003600...) $F=9, S=12$	(0004410...) $F=9, S=4$	(0004420...) $F=10, S=2$	(0005200...) $F=7, S=20$	(0003610...) $F=10, S=6$	(0013300...) $F=7, S=6$	(0013320...) $F=9, S=1$

Lazar, Mason, Macpherson, Srolovitz, *Phy. Rev. Lett.* (2012).

Kinetic theories

Several groups of physicists and materials scientists introduced related, but distinct, kinetic theories at roughly the same time (1988-1993). All these models have the form:

$$\partial_t f_k + (k - 6)\partial_x f_k = \sum_{j=k-1}^{k+1} T_{j,k} f_j, \quad 0 < x < \infty, t > 0.$$

The left hand side describes the evolution of the population of k-gons by the von Neumann-Mullins rule (here x denotes area).

The right hand side describes the "collisions": i.e. the change in population caused by the vanishing of edges or grains.

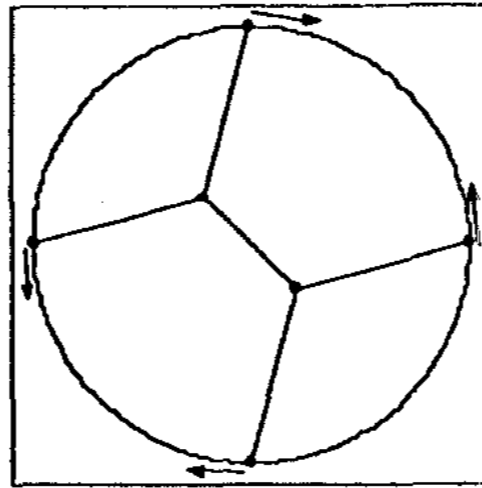
Each kinetic equation reported on here has a different collision term, arising from a different accounting of grain or edge deletion.

Singular events: (1) vanishing of an edge

The vanishing of an edge leads to an unstable 4-vertex and "neighbor switching".

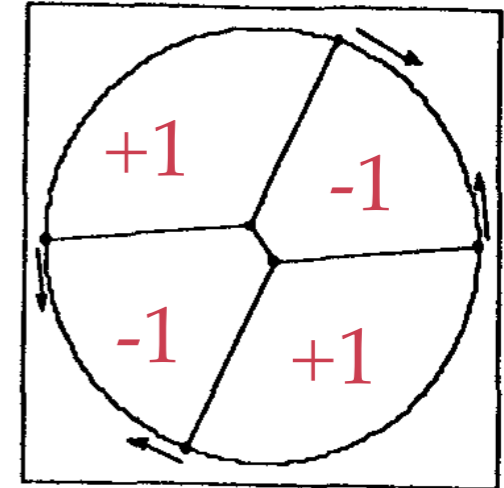
Four cells participate in the switch:
2 gain an edge, 2 lose in edge.

Fig. 1



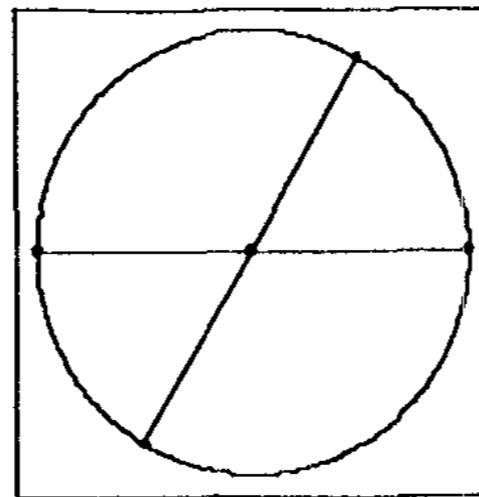
energy: 3.863703

(a)



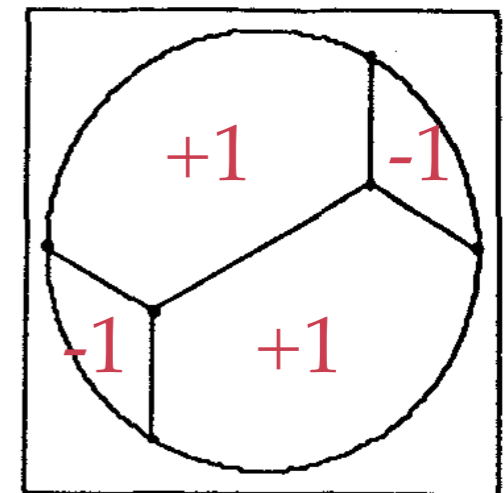
energy: 3.984779

(b)



energy: 4.000000

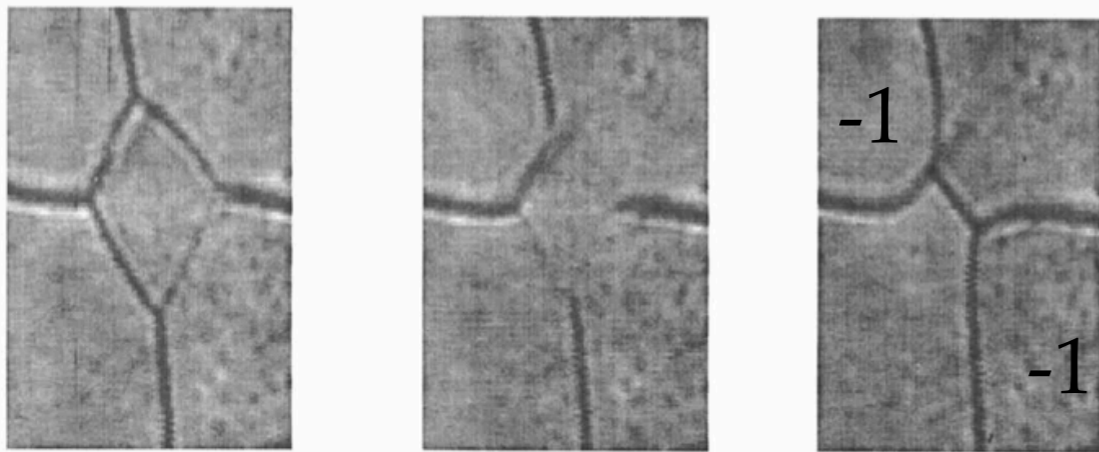
(c)



energy: 3.464102

(d)

Singular events: (2) vanishing of a grain

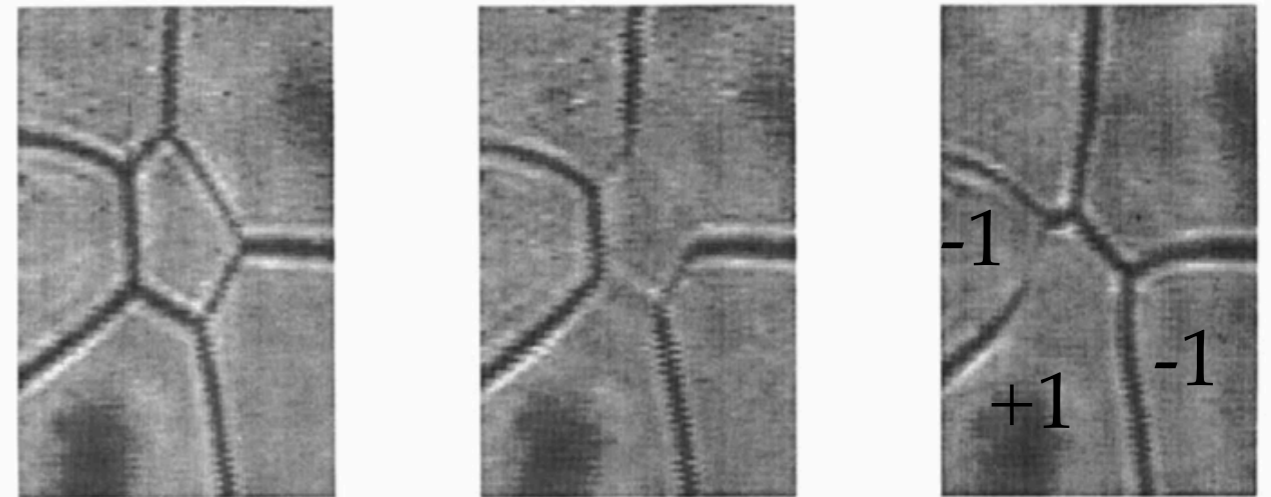


0 sec.

20 sec.

40 sec.

Fig. 4. Shrinking of a 4-sided grain in a 2D SCN-polycrystal.



0 sec.

20 sec.

40 sec.

Fig. 5. Shrinking of a 5-sided grain in a 2D SCN-polycrystal.

Loss of a 4-gon.

2 neighbors lose 1 edge.

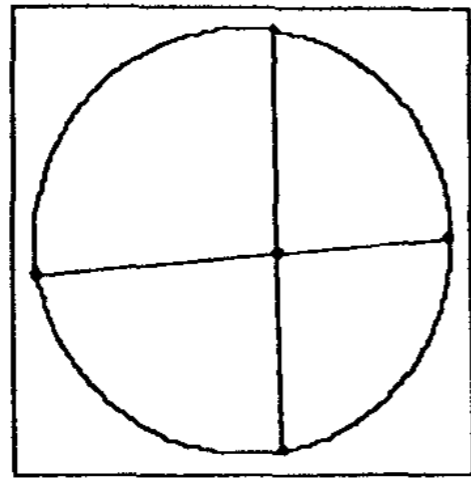
Vanishing of a 5-gon.

2 neighbors lose 1 edge.

1 neighbor gains 1 edge.

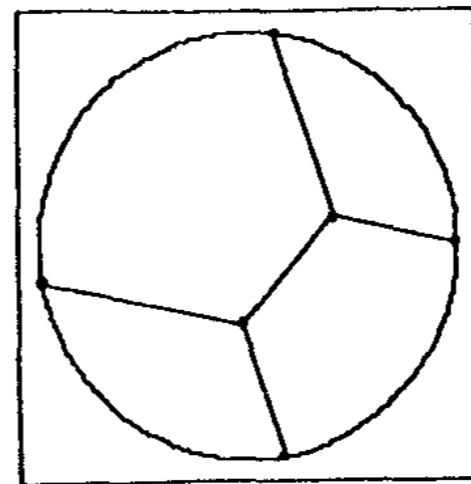
Figures: Fradkov, Glicksman, Palmer, Nordberg, Rajan (Physica A 1993)

Singular events: (3) topological changes in the vanishing of a 4-gon



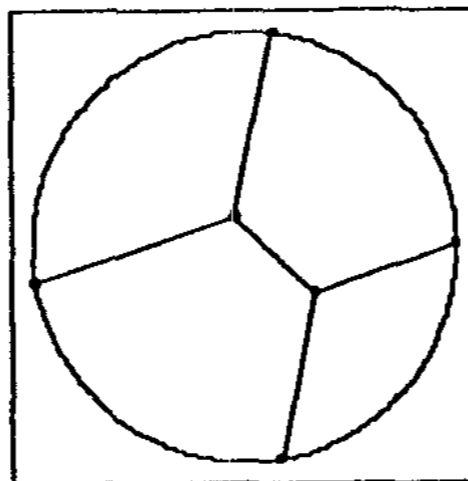
energy: 3.968

(a)



energy: 3.794

(b)

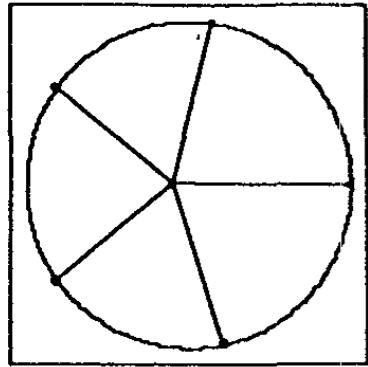


energy: 3.866

(c)

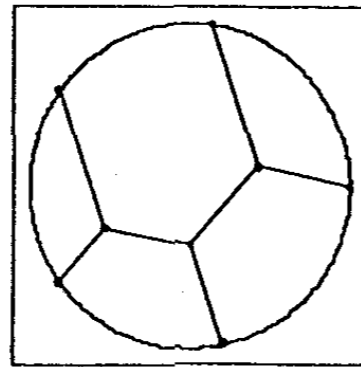
The vanishing of a 4-cell passes through an unstable 4-vertex, and can lead to two topologically distinct networks.

Singular events: (4) vanishing of a 5-gon



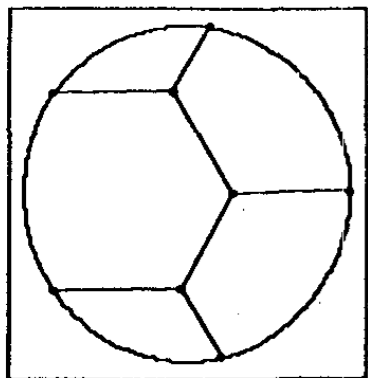
energy: 4.986

(a)



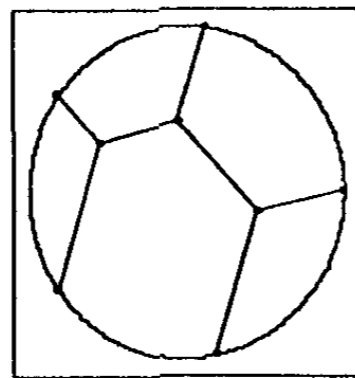
energy: 4.659

(b)



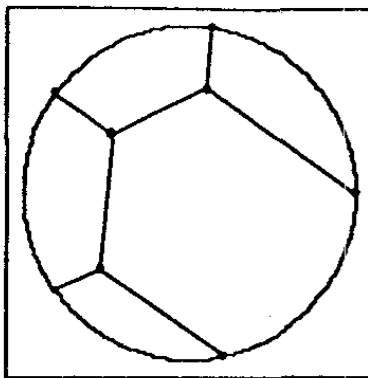
energy: 4.497

(c)



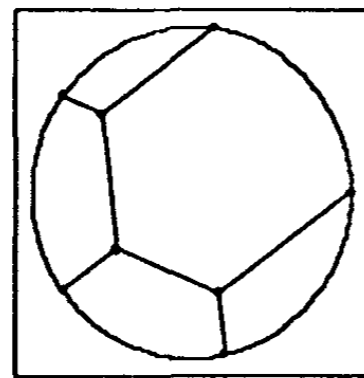
energy: 4.617

(d)



energy: 4.531

(e)



energy: 4.476

(f)

The vanishing of a 5-cell occurs through passage through the unstable 5-vertex and can lead to five topologically distinct networks.

The number of distinct networks is the same as the number of planar, rooted trees with 4 and 5 vertices respectively.

Fig. Fradkov, Magnasco, Udler, Weaire, (Phil. Mag. Lett. 1993).

Common features of kinetic theories

- (a) Mean-field assumption: Ignore correlations between grain shapes. At each singular event, pick grains independently and increase or decrease their number of edges by 1, according to the event type. For example, when a 5-gon vanishes pick three grains independently, decrease the number of edges for two of them, and increase the number of sizes for one of them.
- (b) assume probability of picking a k -gon is proportional to k .
assume probability of picking a k -gon is proportional to total number of k -gons.
- (c) Rate of vanishing events is proportional to number density of k -gons with zero area.
- (d) Total number decreases.
Total area is preserved.
Polyhedral defect is preserved (integral form of Euler characteristic).

Distinct features of kinetic theories

Fradkov-Udler (1994): introduces a phenomenological parameter to parametrize relative rate of vanishing of edges and grains. Ignores vanishing of 5 grains.

Flyvbjerg (1993): ignore vanishing of edges. Obtains a model with no free parameters.

Marder (1987): wants to remove sizes from 2 neighboring face with smallest areas when a 4-gon vanishes. Does this by picking four neighbors independently, and removing edges from the two smaller ones.

Beenakker (1987): assume all faces circular arcs, finds a most likely topology given the perimeter, treats k as a continuous variable, and obtains a diffusion equation.

An example of a kinetic equation (Flyvbjerg)

$$\partial_t f_k + (k - 6) \partial_x f_k = \sum_{j=k-1}^{k+1} T_{j,k} f_j, \quad 0 < x < \infty, t > 0.$$

$$T_{j,k} = \begin{cases} c_+ j, & j = k - 1 \\ \frac{\dot{A}}{A} - (c_+ + c_-) k, & j = k, \\ c_- j, & j = k + 1. \end{cases}$$

$$c_+ = \frac{5}{6} f_5(0, t).$$

$$c_- = \frac{1}{6} \sum_{l=0}^5 (l - 6)^2 f_l(0, t) + c_+.$$

Only nonlinearity is in the coupling terms $f_l(0, t) f_j(x, t)$.

What is the correct kinetic theory?

All equations seem to match experimental data to reasonable approximation...

On the other hand:

- (i) the experimental data is rather limited -- about 1000 soap bubbles in Marder's comparison.
- (ii) others compare with numerical simulations of roughly the same size, but provide no explanation on the numerical resolution of singular events.
- (iii) there appears to be no side-by-side comparison of the various equations to the same data sets.

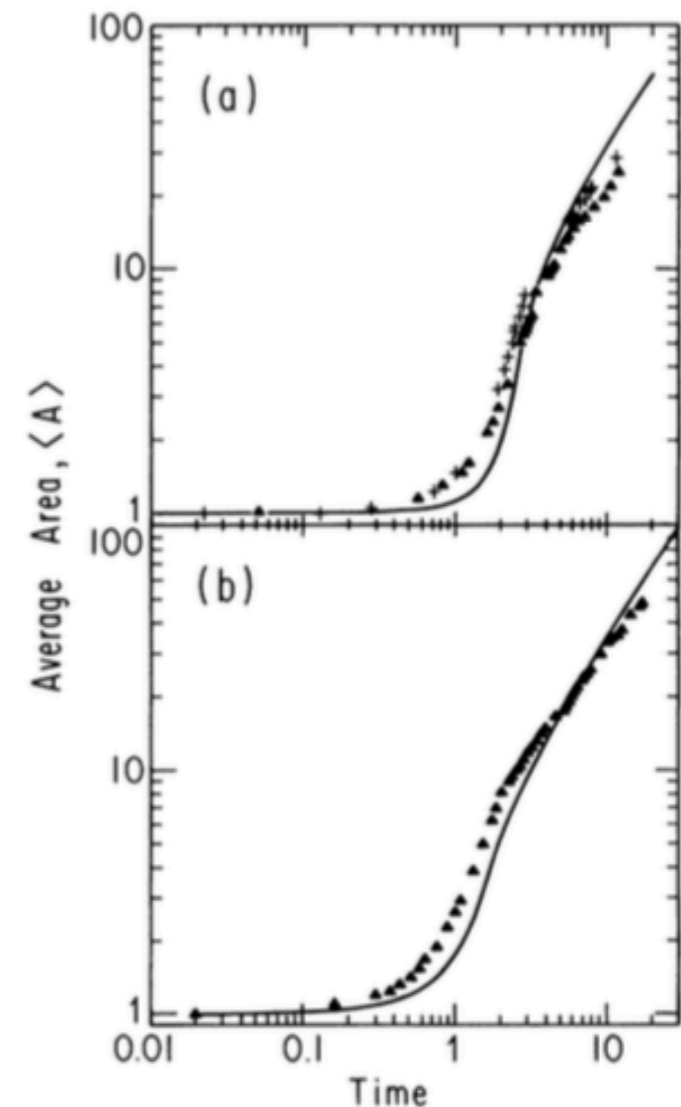


FIG. 3. The average area of bubbles is shown as a function of time. Theory is shown in the solid lines, and data from Ref. 1 in the remaining symbols. The time axes are scaled by measurements of the constant κ appearing in von Neumann's law. In (a) the theory begins with an initial distribution containing 90% six-sided bubbles, 10% an even mixture of fives and sevens. Two experimental runs with a similar initial condition are displayed as well. In (b) are shown theoretical and experimental runs beginning with 80% six-sided bubbles. The theory is fairly insensitive to details of the initial area distributions; these were chosen so as to be close to the conditions of the experiments.

The kinetic equations work as a quick and dirty approach to the problem. However, the "thermalizing" effect of coarsening, depends critically on the flow through singular events, which remains poorly understood. At present, we do not know how to connect solutions to the PDE with the kinetic equations.

But there are many unexplored problems of intermediate difficulty which contain some of the same features. For example, a purely combinatorial description of coarsening, i.e. evolution of a planar graph through discrete elementary moves as shown below, is already interesting.

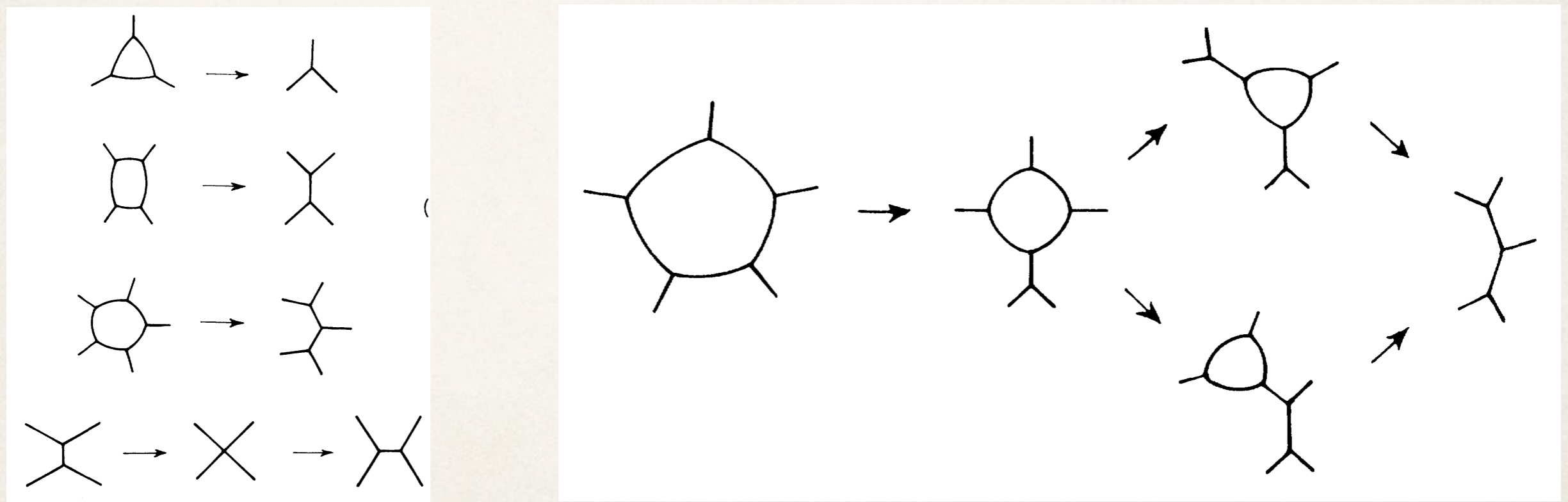
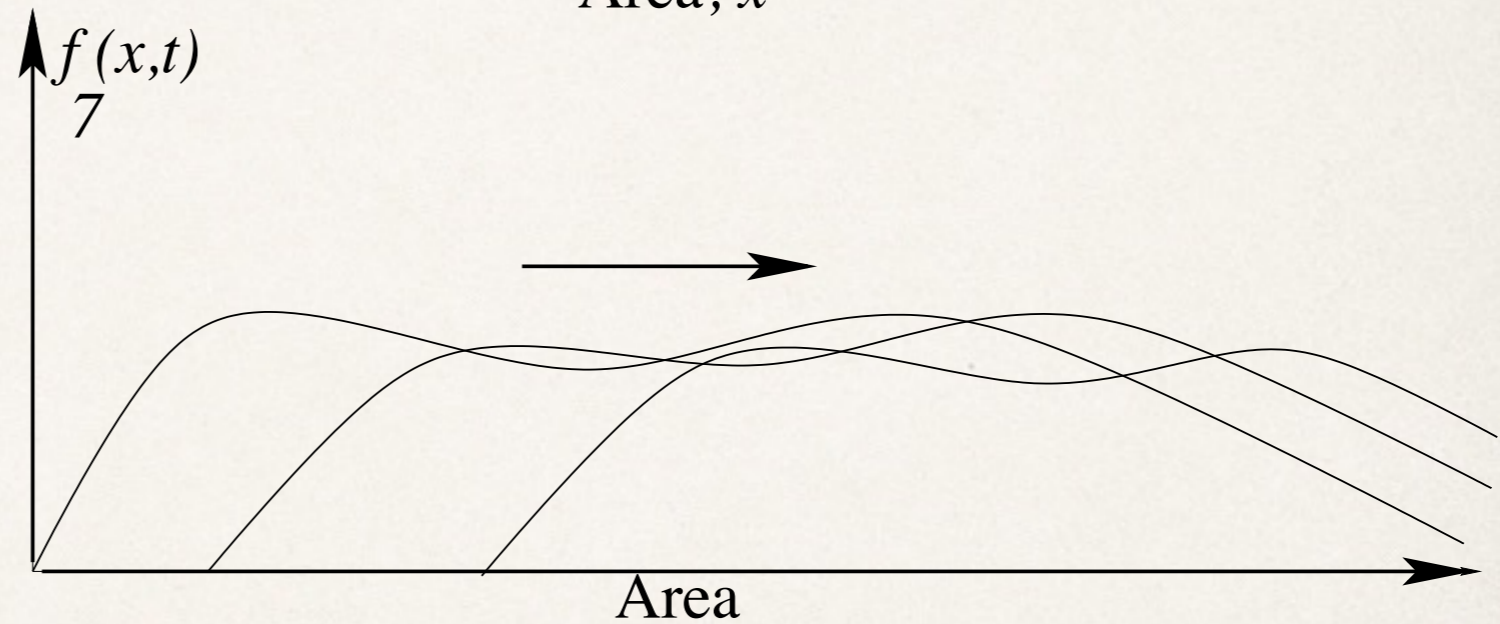
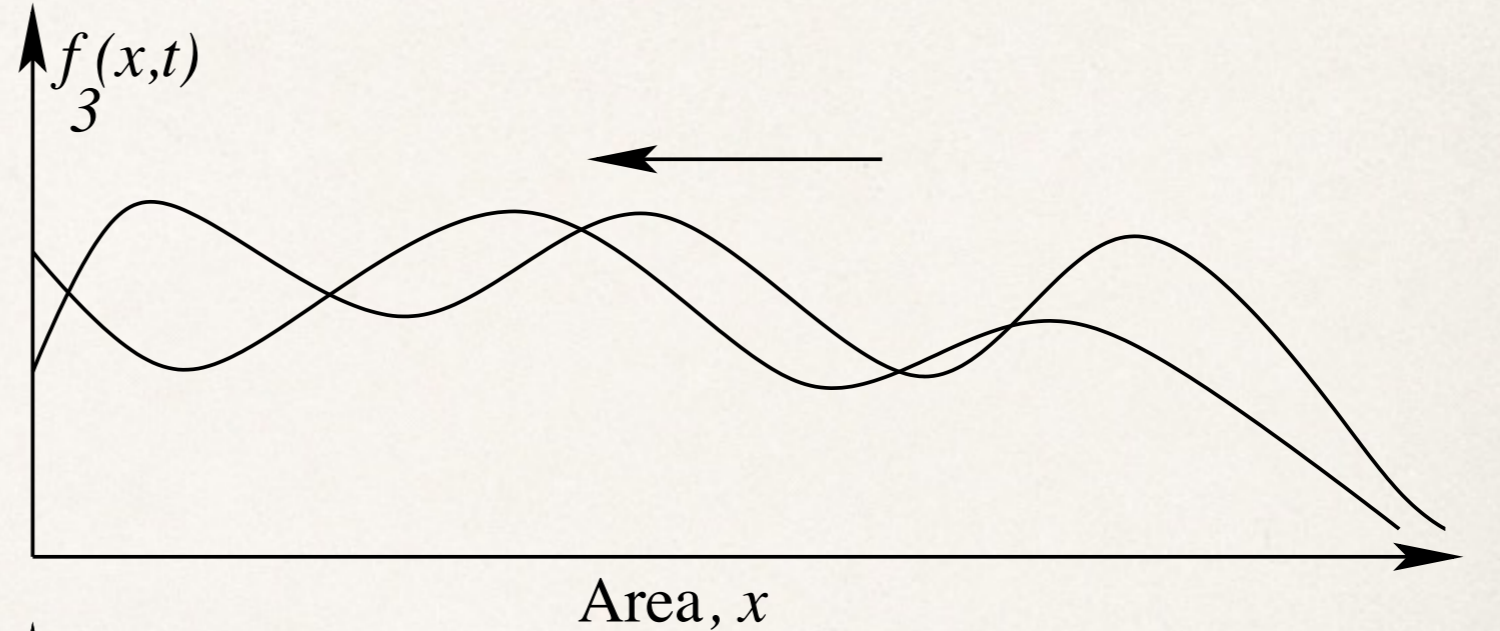
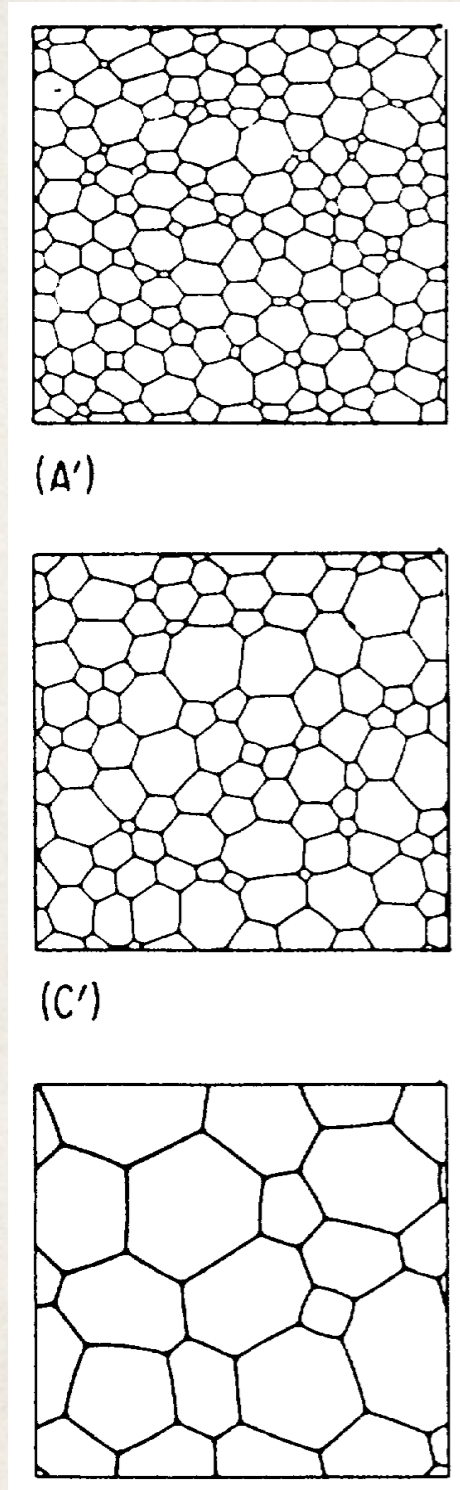


Fig. Flyvbjerg (Phys. Rev. E. 1993).

Random fields compared with kinetic description



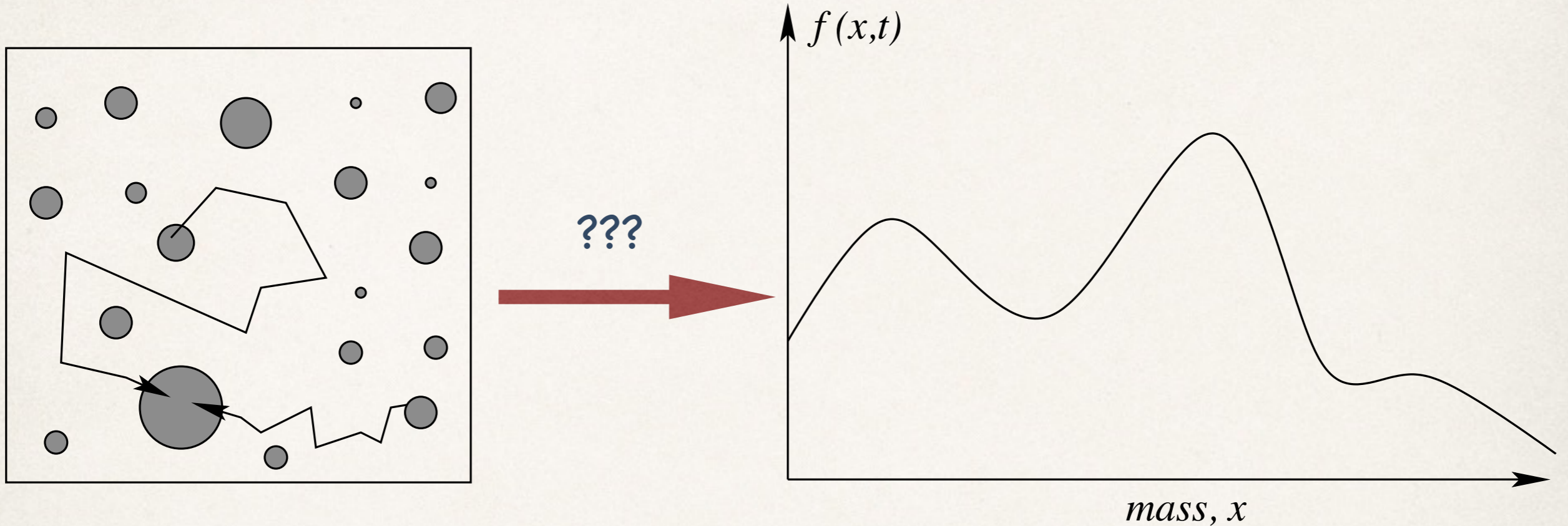
One solution to PDE, from an ensemble of such solutions.

Self-similar infinite networks?

Flow of number densities of 3 and 7 grains

Self-similar solutions to kinetic equations.

Hydrodynamic limits (1): a comparison for coagulation



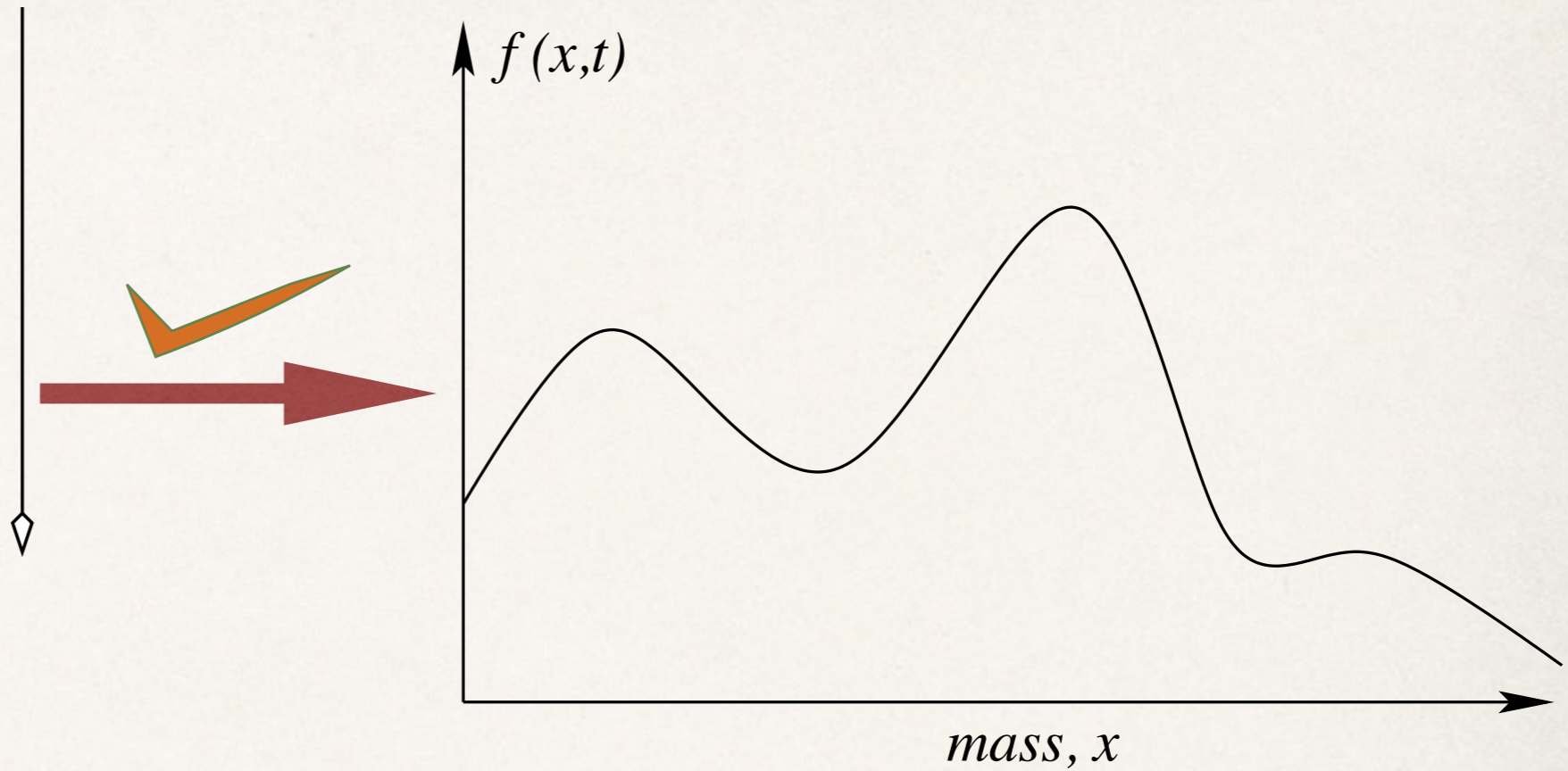
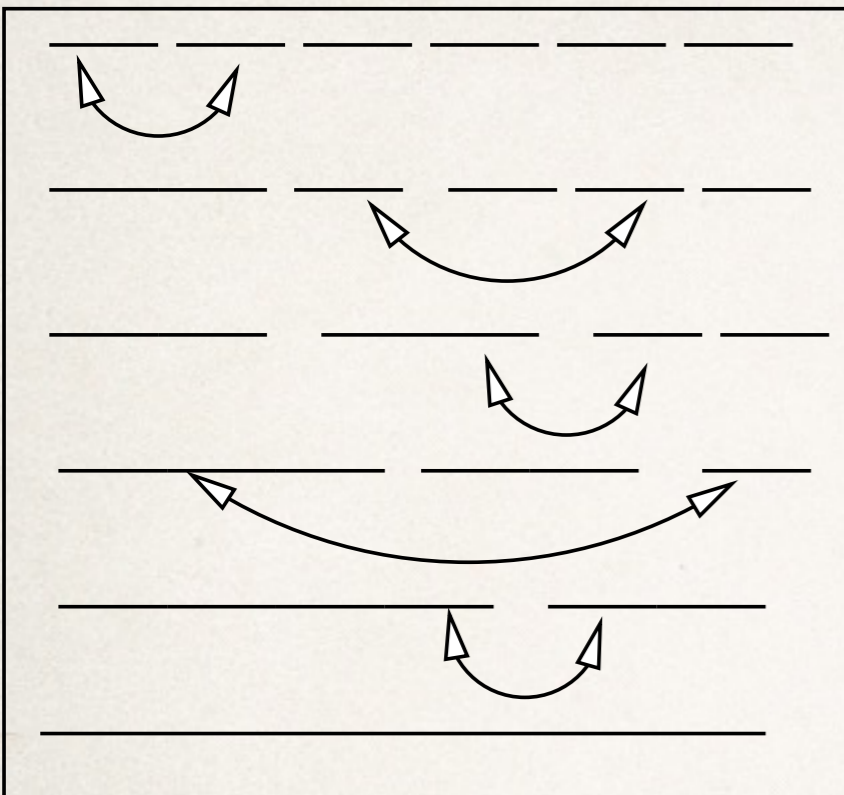
Ensemble of diffusing colloidal particles that stick when they meet.

$$\partial_t f = Q(f, f)$$

$Q(f,f)$ is a binary collision kernel with a rate kernel $K(x,y)$ proposed by Smoluchowski.

Terminology: "Hydrodynamic" refers to origin of this class of problems (derivation of equations for gas dynamics and the Boltzmann equation from hard spheres).

Hydrodynamic limits (2): a comparison for coagulation



Marcus-Lushnikov process:

State space = partitions of $\{1, \dots, N\}$.
Transition rates given by fixed
coagulation kernel $K(x, y)$. The rate
kernel (heuristically) captures all
physics).

$$\partial_t f = Q(f, f)$$

Find a simpler N particle system (Markov process) whose empirical measures satisfy the kinetic equations in the limit of large numbers.

The good and the bad

Bad:

Have removed all geometry. This is not a first principles derivation.

Good:

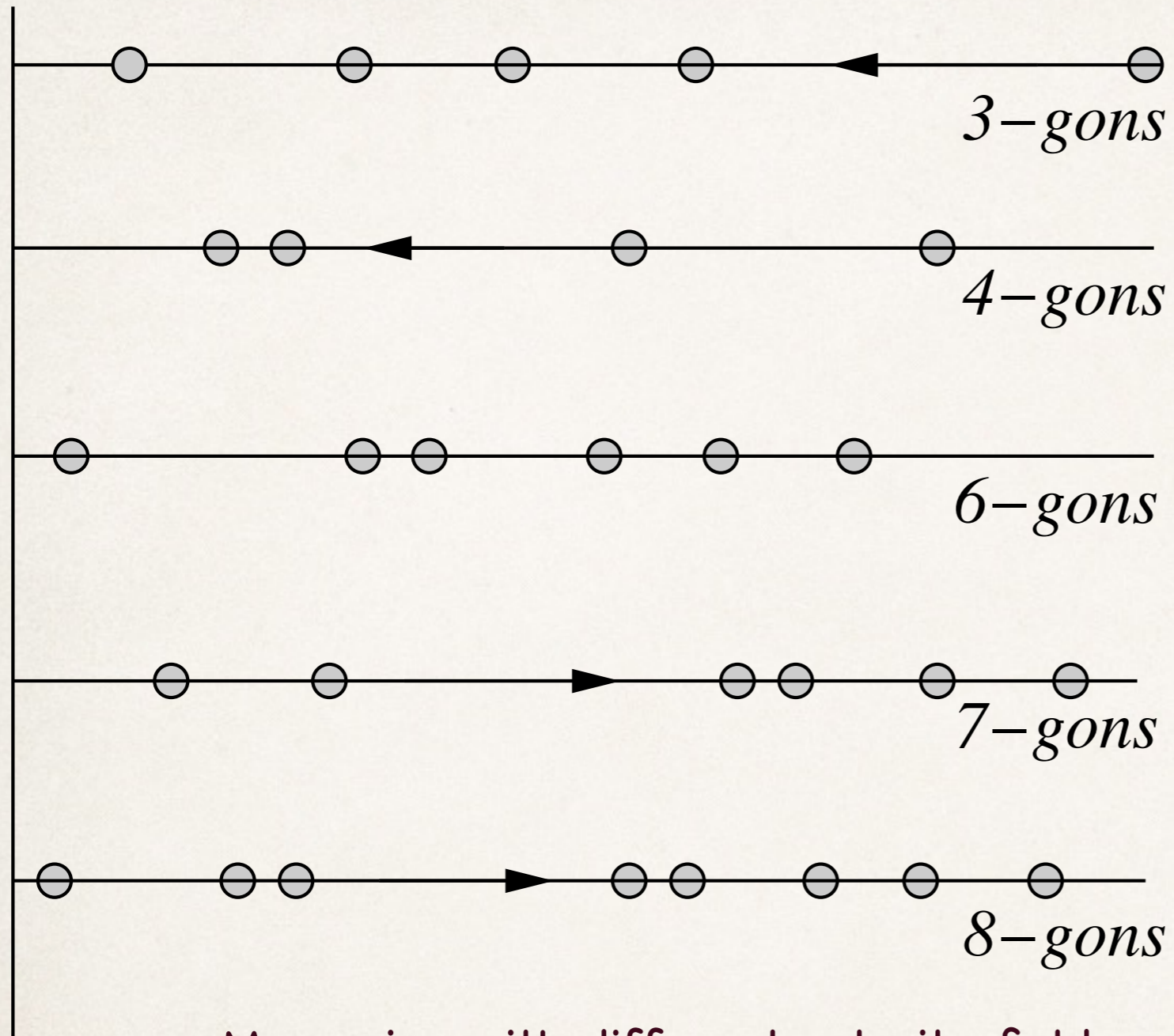
(1) The simplified Markov process clarifies many of the probabilistic assumptions implicit in the kinetic equations.

Technically: basic estimates via martingales.

(2) Abstract structure often leads to connections with other areas and is usually of independent interest.

(3) Some progress, since the geometric evolution of random networks is currently out of reach (no global well-posedness, resolution of singularities).

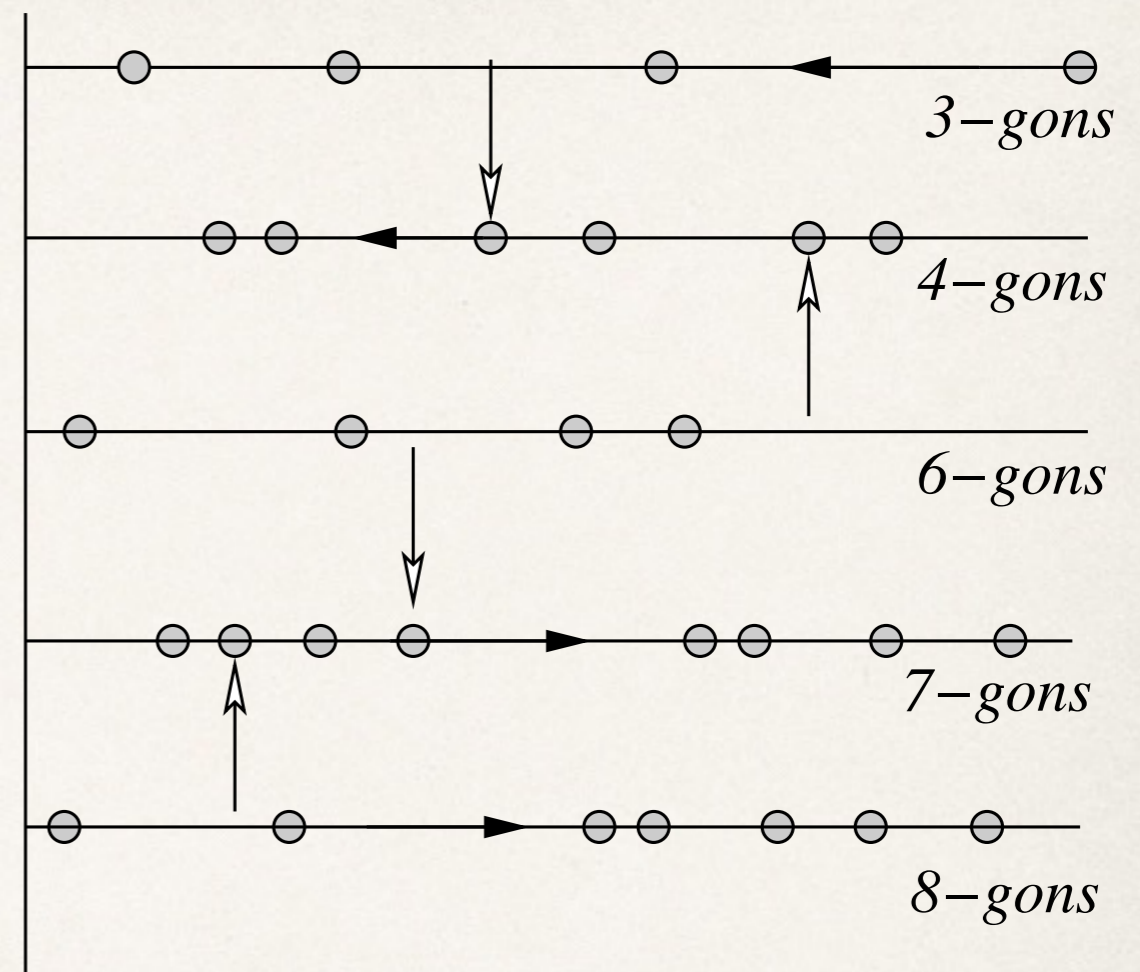
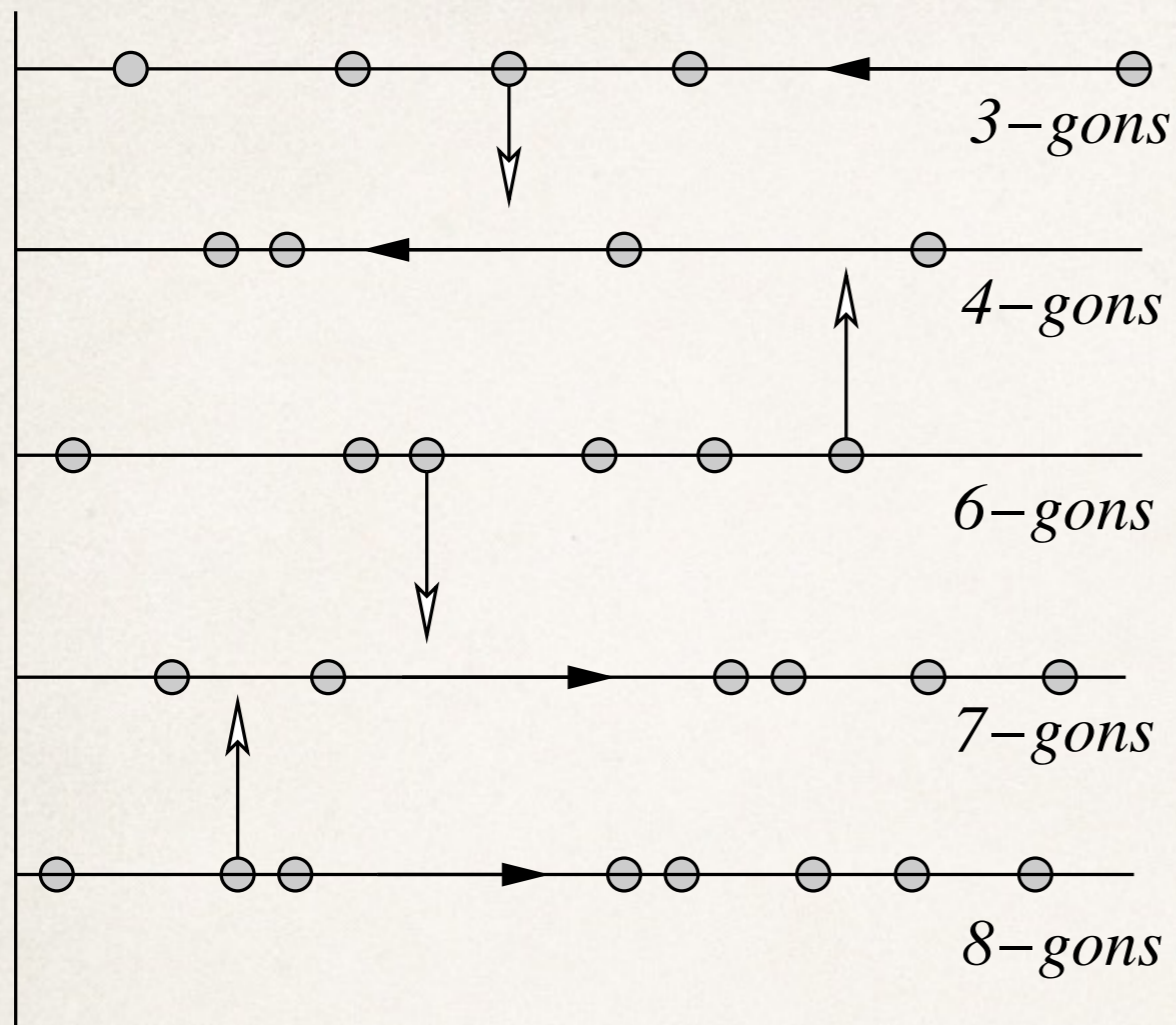
Our particle system



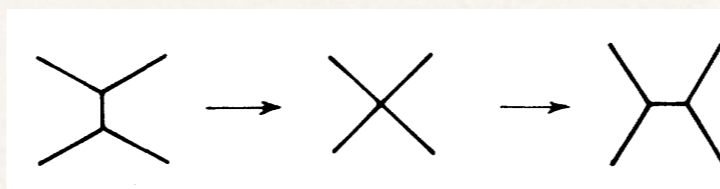
M species with different velocity fields, some left moving, some zero, some right moving. For example, as above.

State of the system = N points with coordinates (s,x) denoting species and size respectively.

Transitions (1). Deletion of edges



Immediately before jump

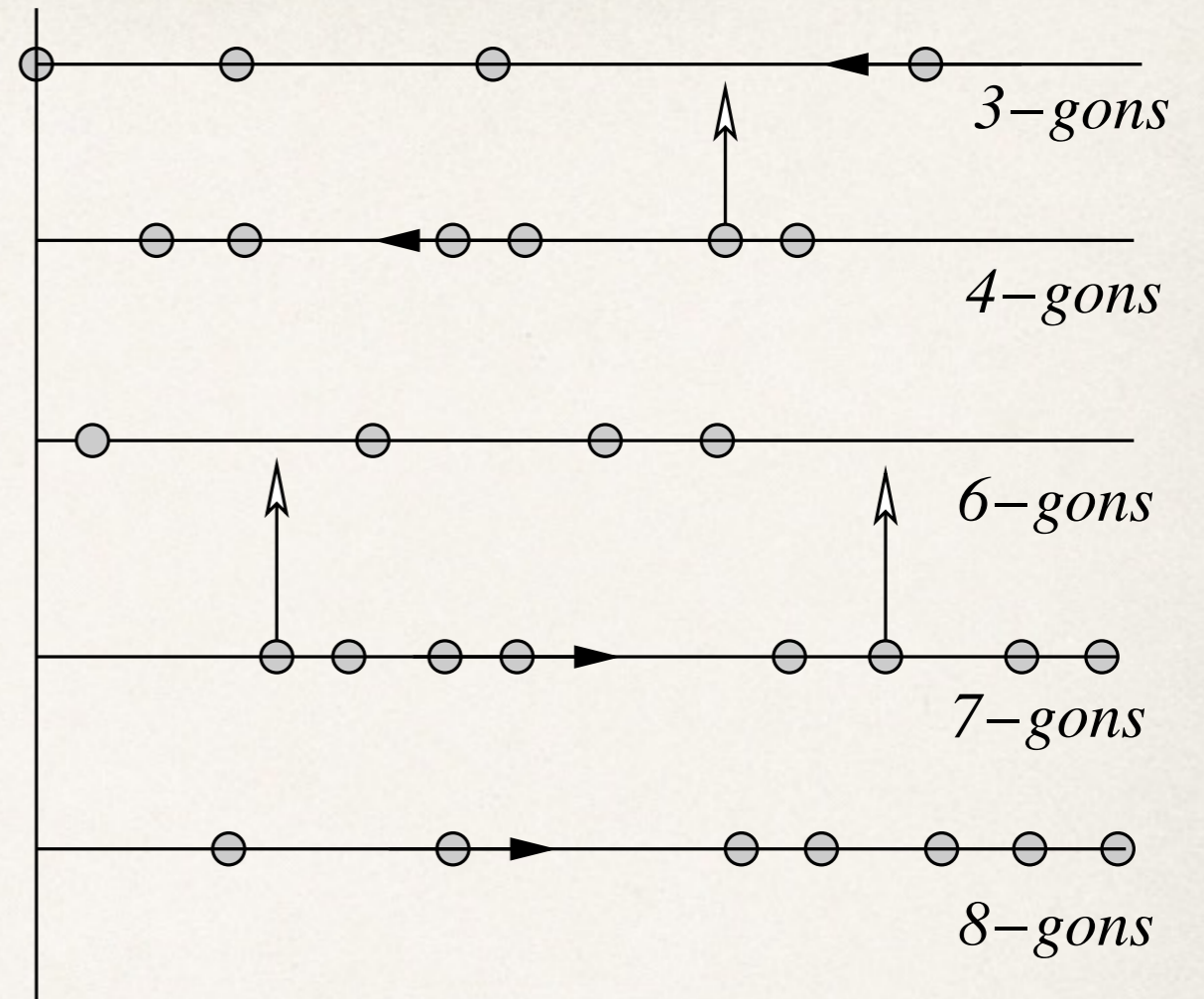
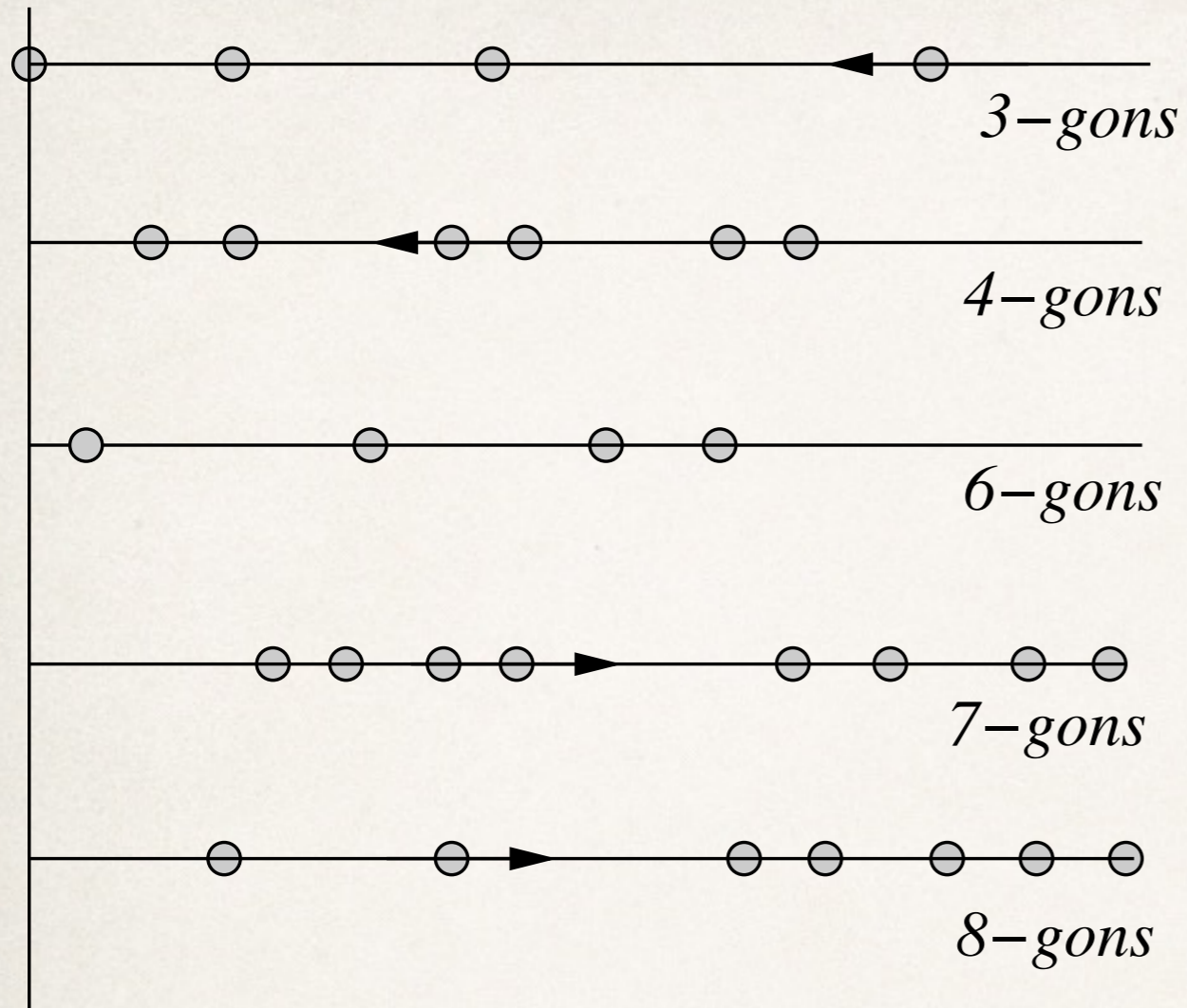


After jump

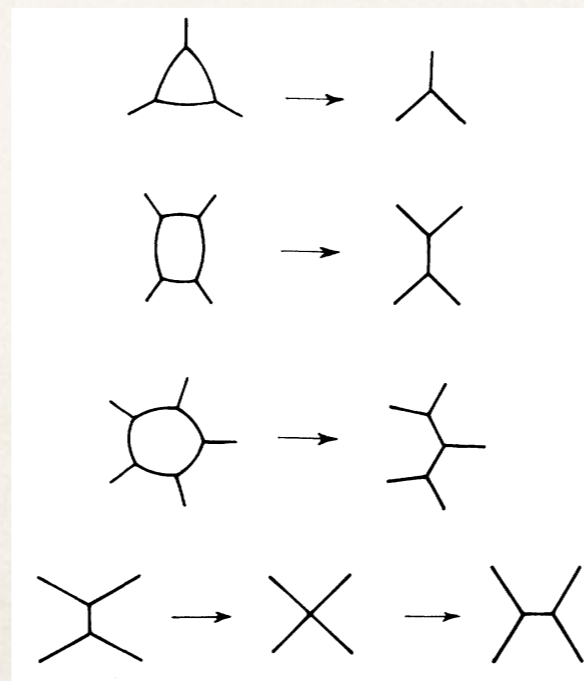
Markovian assumption: Times of jumps are independent, exponential random variables with rate constant that could depend on the state prior to jump.

Mean field: no correlation between neighbors.

Transitions (2). Deletion of grains (boundary events)

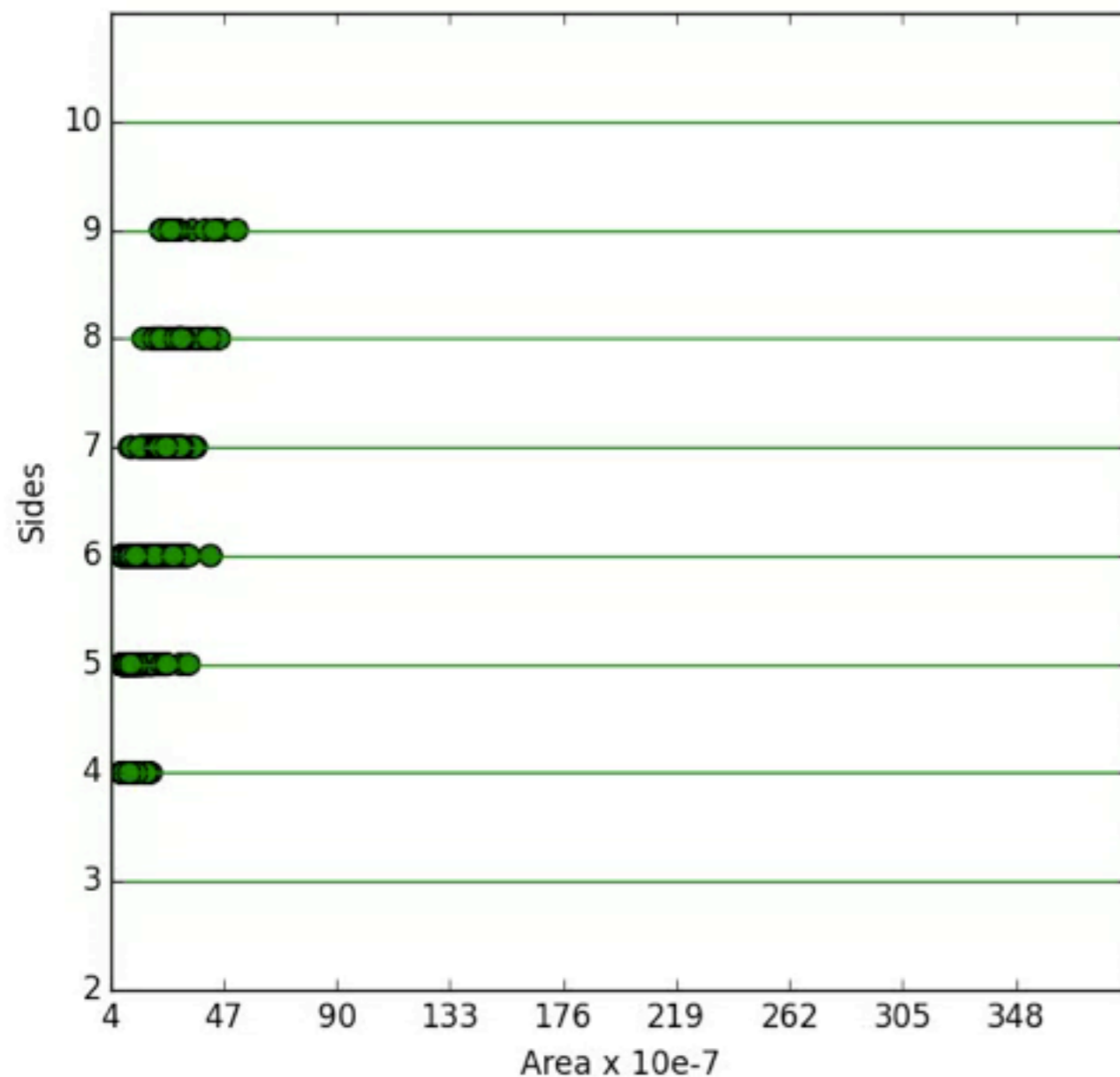


A particle hits the origin
(size becomes zero).



A fixed number of independent
particles are chosen and mutated to
other species. This number depends
on the particular boundary event.

Projecting numerical data to the model



Acknowledgements:

Matt Elsey (computation of grain boundary evolution);
Joe Klobusicky (conversion to particle model).

General model

$\{M_-, M_0, M_+\}$ Number of species that have negative, zero and positive velocity.

$\{v_1, \dots, v_M\}$ Velocity fields (need not be constant).

There are M_- possible boundary events, corresponding to each left moving species (e.g. k-gons with k less than 6).

$K^{(l)}$ Number of particles that mutate at boundary event l (e.g. 3 at 3-gon, 2 at 4-gon, 3 at 5-gon).

$R^{(l)}$ Matrix of size $K^{(l)} \times M$ that takes values in $\{1, \dots, M\}$.
Describes the mutation of species at boundary event at species l .

$w^{(l)}$ A vector of positive weights of length M used to define probabilities (needed to bias selection of k-gons by k).

The law of mutation at boundary events

At a boundary event at species l pick random particles

$$(S_1, X_1), (S_2, X_2), \dots, (S_{K^{(l)}}, X_{K^{(l)}})$$

such that the species S 's are independent, with identical law

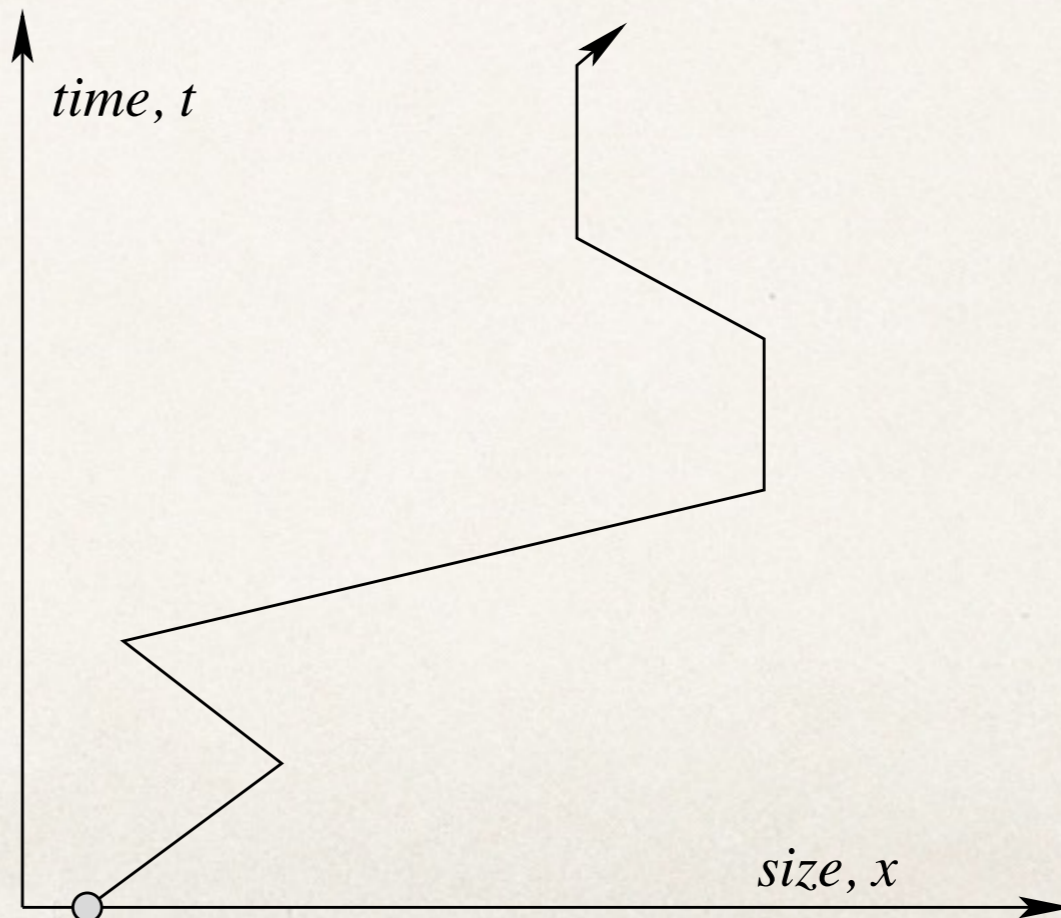
$$\mathbb{P}(S_j = s) = \frac{w(s, l) N_s}{\sum_{k=1}^M w(k, l) N_k}.$$

Each X_j is conditional on the corresponding S_j
and is chosen uniformly from the particles of species S_j

The particle (S_j, X_j) is mutated to $(R_{S_j, j}^{(l)}, X_j)$

General structure: consider only boundary events

- (1) The particle system is an example of a piecewise deterministic Markov process (PDMP). Given the state, the time of the next jump is deterministic. Such systems were typically studied in queuing theory, boundary events correspond to the arrival of customers at a queue.
- (2) The evolution of a tagged particle consists of deterministic drift, with jumps in the velocity caused by mutation between species.



Kinetic equations

$$\partial_t f_\sigma(x, t) + \partial_x(v_\sigma(x) f_\sigma(x, t)) = \sum_{l=1}^M f_l(0, t) v_l(0) \left(-K^{(l)} W_\sigma^{(l)}(t) f_\sigma(x, t) + \sum_{k=1}^M W_k^{(l)}(t) f_k(x, t) \sum_{j=1}^{K^{(l)}} \mathbf{1}_{\{R_{kj}^{(l)} = \sigma\}} \right)$$

$$W_k^{(l)}(t) = \frac{w_k^{(l)}}{\sum_{p=1}^M w_p^{(l)} F_p(t)}$$

$$F_k(t) = \int_0^\infty f_k(x, t) dx, \quad F(t) = \sum_{k=1}^M F_k(t),$$

The empirical measures

N

The total number of particles (does not change in time).

$(s_1(t), s_2(t), \dots, s_N(t); x_1(t), \dots, x_N(t))$ The state of the system.

I

An open interval on the half-line.

$$\mu_{\sigma, N}(t) \stackrel{\text{def}}{=} \frac{1}{N} \sum_{j=1}^N \mathbf{1}_I(x_j(t)) \mathbf{1}_{\sigma}(s_j(t)).$$

This is the normalized number of particles of species σ in the interval I .

$L_{\sigma, N}(t)$

Normalized number of particles of species σ lost at the origin.

Global semiflow (well-posedness)

Thm. 1. Assume given bounded, continous number densities for each species, such that

$$0 \leq f_\sigma(x, 0), \quad \int_0^\infty f_\sigma(x, 0) dx < \infty, \quad 1 \leq \sigma \leq M.$$

Then the kinetic equation has a unique global solution in $C([0, \infty), (BC \cap L^1)^M)$ and the solution depends continuously on the initial data.

Corollary 1. For initial measures with densities as above, the kinetic equations define a global semiflow in the space of measures equipped with the weak topology.

Remark: This theorem is not optimal when $M=1$. It is possible to define global measure-valued solutions, without assuming the existence of a density. Related to Menon-Niethammer-Pego (2009) on min-driven coagulation.

Convergence in probability

Thm. 2. Assume given bounded, continuous number densities for each species such that

$$0 \leq f_\sigma(x, 0), \quad \int_0^\infty f_\sigma(x, 0) dx < \infty, \quad 1 \leq \sigma \leq M.$$

Consider the N-particle system with initial empirical measures $\mu_\sigma^N(0)$ that converge weakly to the measure $\mu_\sigma(0)$ with density $f_\sigma(0)$.

Then for each $\epsilon > 0$ and $T > 0$:

$$\lim_{N \rightarrow \infty} \mathbb{P} \left(\sup_{0 \leq t \leq T} \max_{1 \leq \sigma \leq M} d \left(\mu_\sigma^N(t), \mu_\sigma(t) \right) > \epsilon \right) = 0.$$

Here d is a distance that metrizes weak convergence of the empirical measures and $\mu(t)$ denotes the solution to the kinetic equations with the given initial data.

Remark: We expect, but have not proved, large deviation bounds for the rate of convergence even in the case $M=1$.

The main estimate for tightness

$$m_N(t, \delta) = \sup_{I, |I| < \delta} \sum_{s=1}^N \mu_{s,N}(t)(I).$$

$$\mathbb{E}(m_N(t, \delta)) \leq C(T) \mathbb{E}(m_N(0, \delta)), \quad t \in [0, T].$$

